

Cytochemical, Structural and Ultrastructural Characterization of Tetrasporogenesis in *Bostrychia radicans* (Ceramiales, Rhodophyta) from the Mangroves of Itacorubi and Rio Ratonés, Santa Catarina, Brazil

Ticiane Rover^{1,2}, Carmen Simioni^{1,2*}, Luciane Cristina Ouriques^{1,2},
Zenilda Laurita Bouzon^{1,2}

¹Department of Botany, Federal University of Santa Catarina (UFSC), Trindade, Florianópolis, Brazil

²Department of Cell Biology, Embryology and Genetics, UFSC, Florianópolis, Brazil

Email: *carmensimioni@hotmail.com

Received 12 December 2013; accepted 21 September 2015; published 24 September 2015

Copyright © 2015 by authors and Scientific Research Publishing Inc.

This work is licensed under the Creative Commons Attribution International License (CC BY).

<http://creativecommons.org/licenses/by/4.0/>



Open Access

Abstract

Little is known about the morphology and location of macromolecules, especially proteins and carbohydrates, in vegetative and reproductive structures of mangrove species, including *Bostrychia radicans*. Therefore, to gain a better understanding of tetrasporogenesis in *B. radicans*, cytochemical, structural and ultrastructural analyses were performed. Thalli were collected from mangroves in Florianópolis, Santa Catarina, Brazil. Fertile branches were fixed and processed for light microscopy (LM), confocal microscopy and transmission electron microscopy (TEM) observations. The LM sections were stained with toluidine blue, periodic acid-Schiff and Coomassie brilliant blue. Tetrasporogenesis occurs in the pericentral cells of the terminal branches. This process is initially characterized by an increase in cell volume, resulting from the proliferation of organelles. The young tetrasporangia remain connected to the basal cell by pit connections. After a considerable increase in volume, the tetrasporocytes divide tetrahedrally, giving rise to haploid spores. During this process, there is an increasing production of starch grains, causing the organelles to group. As the organelles proliferate, the plasma membrane undergoes simultaneous invaginations toward the tetrasporangium center. The most conspicuous organelle throughout tetrasporogenesis was the Golgi complex. Polysaccharidic components are predominant in the tetrasporangium cell wall

*Corresponding author.

throughout tetrasporogenesis. Although protein components prevail in the cytoplasm of younger tetrasporangia, there is a predominance of reserve material with maturation. In the initial phase, there is an increase in the number of chloroplasts and a significant increment of Golgi bodies which contribute to the formation of the amorphous portion of the cell wall and possibly the biosynthesis of starch grains.

Keywords

Bostrychia radicans, Cytochemistry, Tetraspores, Tetrasporogenesis, Ultrastructure

1. Introduction

The characteristics of mangrove ecosystems, such as thin sediment and low oxygen level, cause typical mangrove fanerogams to develop such adaptations as, for example, pneumatophores. These structures allow plants to survive and establish sessile organisms such as algae. These structures are often covered with macroalgae, especially Rhodophytes, as shown by [1], for Brazilian mangroves.

Among the algae occurring in mangroves, the genus *Bostrychia* stands out, particularly the dominant species known as *Bostrychia radicans* (Montagne) Montagne [2]. This species has already been the subject of several studies, including those of [3] and [4], who reported on hybridization. These authors compared different ecotypes of *Bostrychia* isolated from distinct communities. A proteomic comparison of eight complexes isolated from *B. radicans* was also performed by [5], while [6] assessed molecular and reproductive diversity. The authors considered the phylogenetic analysis of plastids and data on the mitochondrial DNA sequences which revealed the existence of seven different evolutionary lineages among samples all around the world.

The red algae exhibit complex reproductive systems and life histories. Post-fertilization development is the basis for classification in the red algae. *B. radicans* reproduces both sexually and asexually. Its fertilization is followed by two asexual generations that produce diploid and haploid spores, termed carposporophytic and tetrasporophytic phases, respectively [7].

Histochemical studies have shown the presence of different molecules which are distributed in a heterogeneous way over distinct cell portions. In seaweed, polysaccharides have been demonstrated to serve many functions as structural components [8] [9]. [10] and [11] showed the occurrence of a positive reaction of the cell wall of *Hypnea musciformis* (Wulfen) J. V. Lamour when stained with toluidine blue, indicating the presence of acidic groups. [12] histochemically compared the reproductive and vegetative tissues of *H. musciformis* and *Halarachnion ligulatum* (Woodward) Kützing. Among investigators reporting the histochemical results of algae reproduction, we highlight [13] who described tetrasporogenesis in *H. musciformis*.

Among the studies reporting on the ultrastructure of red algae tetrasporogenesis are in *Levringiella gardneri* (Sterchell) Kylin [14]; in *Ptilota hypnoides* Harvey [15]; in *Palmaria palmata* (L.) O. Kuntze [16] [17]; in *Erythrocytis montagnei* (Derbès and Solier) Silva [18]; in *Hildenbrandia* Nardo [19]; in *Haloption cuvieri* (J. V. Lamourex) H. W. Johansen & P. C. Silva [20]; in *Chondria tenuissima* (Withering) C. Agardh [21]; in *Osmundea spectabilis* var. *Spectabilis* [22]; and in *Rhodymenia californica* var. *attenuata* (E.Y. Dawson) E.Y. Dawson [23].

Although several structural and ultrastructural aspects of sporogenesis have been studied in a few groups within Ceramiales [20] [21], little is known about the morphology and location of macromolecules, especially proteins and carbohydrates, in vegetative and reproductive structures of mangrove species, including *B. radicans*. Therefore, using cytochemical, structural and ultrastructural analysis, this study aimed to describe and characterize the process of tetrasporogenesis in *B. radicans* stichidia.

2. Material and Methods

Tetrasporophytic thalli of *B. radicans* were collected in the Itacorubi and Rio Ratones mangroves, which are located in Florianópolis, Santa Catarina, Brazil. The fertile portions, called stichidia, were processed for light and transmission electron microscopy.

2.1. Light Microscopy (LM)

For light microscopy, the stichidia were fixed overnight in 2.5% paraformaldehyde in 0.2 M phosphate buffer (pH 7.2). Subsequently, the samples were dehydrated in increasing series of ethanol aqueous solutions. After dehydration, the samples were embedded in historesin (Leica Historesin, Heidelberg, Germany), according to [24]. Sections 5 μm thick were stained using different cytochemical techniques, as described below, and observed and photographed under an Epifluorescent Olympus BX 41 microscope equipped with Image Q Capture Pro 5.1 Software (Qimaging Corporation, Austin, TX, USA). For morphological observations of the tetrasporogenesis process, the sections were stained with 0.5% aniline blue.

2.2. Cytochemical Techniques

LM sections were stained with 1% Periodic Acid-Schiff (PAS) used to identify neutral polysaccharides [25]; 0.5% Toluidine Blue (TB-O) (pH 4.4) [26] to identify acid polysaccharides recognized through their characteristic metachromatic reaction; and 0.02% Coomassie Brilliant Blue (CBB) in Clarke's solution to identify proteins [25]. Controls consisted of applying solutions to sections without the staining component (e.g., omission of periodic acid application in the PAS reaction). Also, 10% Alcian Blue (AB) (pH 0.5) and 10% Alcian Yellow (AY) (pH 2.5) were used for acid polysaccharides (sulfate and carboxylate, respectively) [27].

2.3. Confocal Microscopy

For observations under the confocal microscope, stichidia were transferred to Eppendorf tubes, and a solution of detergent (Triton X-100) was added to increase the permeability of the membrane, followed by the addition of DAPI (4',6-diamidino-2-phenylindole) at a concentration of 0.5 $\mu\text{g}\cdot\text{mL}^{-1}$ in distilled water for 50 minutes [28]. For observations of cell wall structure of stichidia, calcofluor was added at a concentration of 20 $\mu\text{g}\cdot\text{mL}^{-1}$ for 30 minutes. The material was mounted on slides and sealed using colorless nail polish. Observation and images were made under confocal microscopy (Leica DMI 6000 B) at the Central Laboratory of Electronic Microscopy (LCME), Universidade Federal de Santa Catarina. Nuclei were observed at 405 nm laser wavelength excitation with emission spectrum from 510 to 566 nm. Chloroplast autofluorescence was observed at 488 nm laser wavelength excitation with emission spectrum from 639 to 701 nm [29]. The cell wall structure was observed at 440 nm laser wavelength excitation with emission spectrum from 437 - 490 nm.

2.4. Transmission Electron Microscopy (TEM)

For observations under the transmission electron microscope (TEM), stichidia were fixed overnight in 2.5% glutaraldehyde buffered with 0.1 M sodium cacodylate (pH 7.2) plus 0.2 M sucrose. Post-fixation for 6 h in 1% osmium tetroxide was followed by dehydration with a graded acetone series, and thus the material was embedded in Spurr's resin. Ultra-thin sections were stained with aqueous uranyl acetate followed by lead citrate, according to [30]. The samples were then examined under a Jeol JEM1011 electron microscope operating at 80 kV.

3. Results

3.1. Light Microscopy

The tetrasporophyte of *B. radicans* (Montagne) Montagne consists of a cylindrical and ecorticated thallus, abundantly branched with an alternating arrangement and a polysiphonic organization (Figure 1(a) and Figure 1(b)). At the apex of branches, the pericentral cells differentiate into tetrasporangia (Figure 1(a)). As a result, this region, which constitutes the stichidia, becomes dilated and densely pigmented (Figure 1(a)). In this region, through mitosis, the pericentral cells give rise to two other cell types: the basal cell and the young tetrasporangium (Figure 1(c)). Early in the maturation process, the young tetrasporangia are characterized by an increase in cell volume, resulting from intense organelle proliferation, which gives a dense aspect to the cytoplasm. At the initial phases, the young tetrasporangia remain connected to the basal cell by pit connections (Figure 1(c)). After a considerable increase in volume, tetrasporangia undergo meiosis, dividing tetrahedrally, subsequently giving rise to four uninucleate tetraspores (Figure 1(d)).

The beginning of tetrasporogenesis was characterized by the deposition of acidic mucilaginous material in the

cell wall in the young tetrasporangia (**Figure 1(e)**). To understand the nature of this mucilage, tetrasporangia were stained with AT-O at various maturation stages, and a characteristic metachromatic reaction in the cell wall matrix revealed the polysaccharidic composition of this region (**Figures 1(e)-(g)**). While the cytoplasm of the

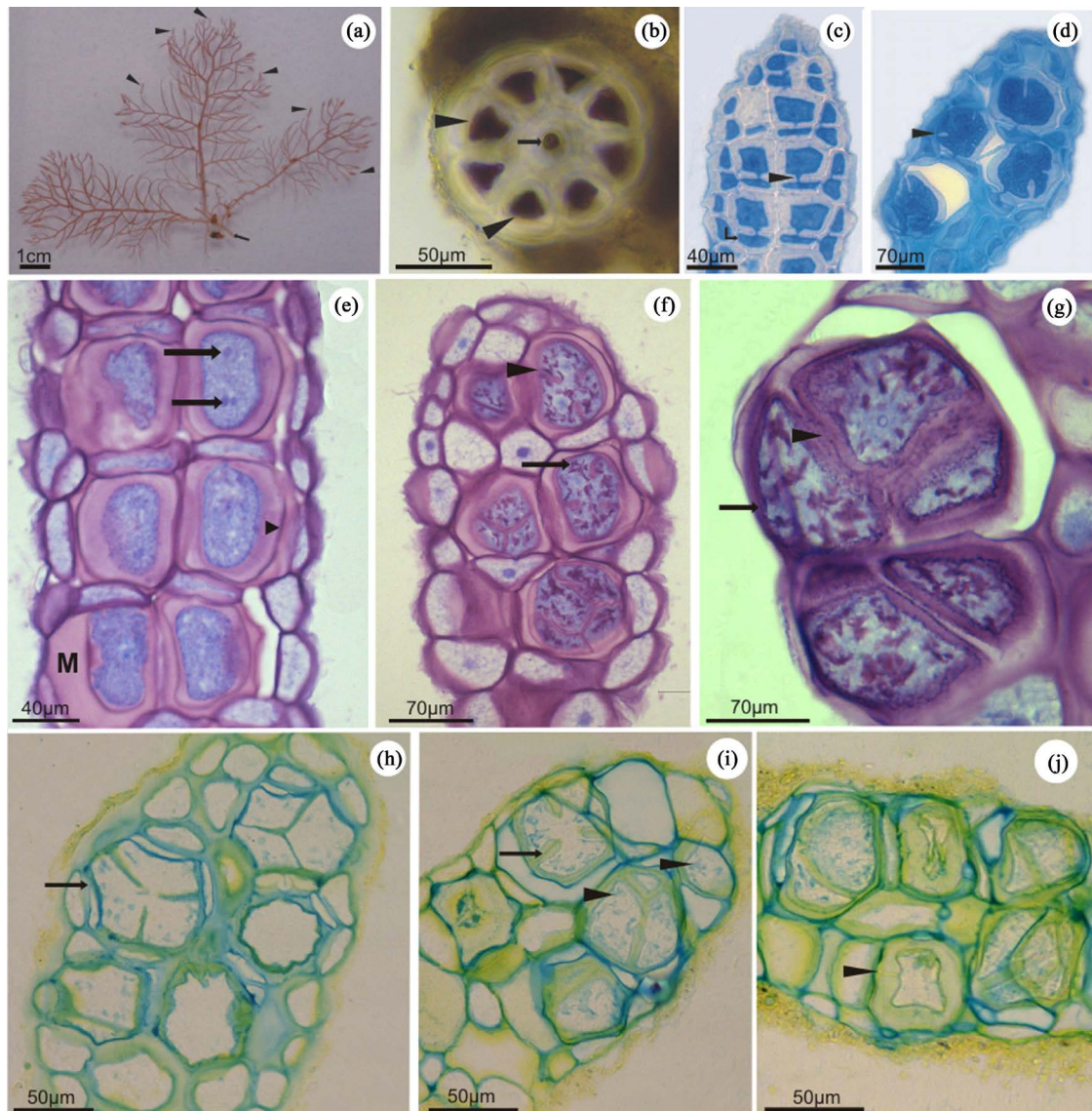


Figure 1. Light microscopy of *Bostrychia radicans*. (a) Tetrasporophytic thallus showing several stichidia in the terminal branches (arrowheads). (b) Cross section of the thallus exhibiting the polysiphonic organization. The arrow indicates the central cell, and the arrowheads point to the pericentral cells. (c)-(d) Longitudinal sections of stichidia stained with aniline blue. (c) Beginning of tetrasporogenesis. Note that the daughter cells remain connected to the basal cells (arrow) by pit connections (arrowhead). (d) Cell dividing tetrahedrally (arrowhead). (e)-(g) Longitudinal sections of *B. radicans* stichidia stained with TB-O. (e) Stichidia with young tetrasporangia surrounded by a thick mucilage (M). Note the presence of one or more nuclei per cell (arrows). The cell walls presented metachromatic reaction (arrowhead). (f) Longitudinal section showing incomplete cell division of the tetrasporangia (arrowhead). Arrow points to the metachromatic granulations in the cytoplasm. The cell walls exhibit metachromatic reaction. (g) Tetrasporangia at the end of the maturation process showing complete cell division (arrowhead). The cell walls stained metachromatically (arrow). (h)-(j) Longitudinal sections of stichidia treated with AB and AY. (h) Dividing tetrasporangium revealing a positive reaction to AB in the cell wall (arrow). (i) Tetrasporangium in the process of maturation, showing positive reaction of the cell walls and invaginations (arrow) when stained with AB and AY. Note the positive reaction of the cytoplasmic granules to AB (arrowheads). (j) Tetrasporangia at various maturation stages presenting positive reaction to AB in the inner cell walls and to AY in the outermost layer of the cell wall. Note a young tetrasporangium connected to its basal cell by a pit connection (arrowhead).

young tetrasporangia showed a homogeneous orthochromatic reaction to TB-O (Figure 1(e)), metachromatic granulations gradually appeared throughout the cytoplasm with maturation (Figure 1(f)).

When treated with AB, the cell wall of all *B. radicans* stichidia cells showed an intense reaction (Figure 1(h)). During cytokinesis, concomitant with the plasma membrane invagination process, the deposition of a cell wall rich in sulfated polysaccharide was observed through its positive reaction to AB (Figure 1(i)). Cytoplasmic granules were also stained with AB (Figure 1(i)). These results corroborate those observed for TB-O, reinforcing the finding that polysaccharide sulfation occurs intracellularly. Sections treated with AY showed positive reaction surrounding all tetrasporangia, also indicating the presence of carboxylated polysaccharides as a mucilage component (Figure 1(j)).

When stained with PAS, the tetrasporangia cell walls revealed a weak reaction, indicating the presence of neutral polysaccharides, probably cellulose (Figure 2(a)). On the other hand, tetrasporangia during maturation showed progressive cytoplasmic activity, mainly related to the synthesis of reserve material (floridean starch grains). In young tetrasporangia, this synthesis was reduced, as evidenced by the low amount of PAS-positive granulations observed (Figure 2(a)). Mature tetrasporangia showed a densely stained cytoplasm denoting a significant increase in the production of floridean starch grains (Figure 2(b) and Figure 2(c)).

The main constituents of cellular organelles are proteins. They are also present in the cytoplasm as molecules

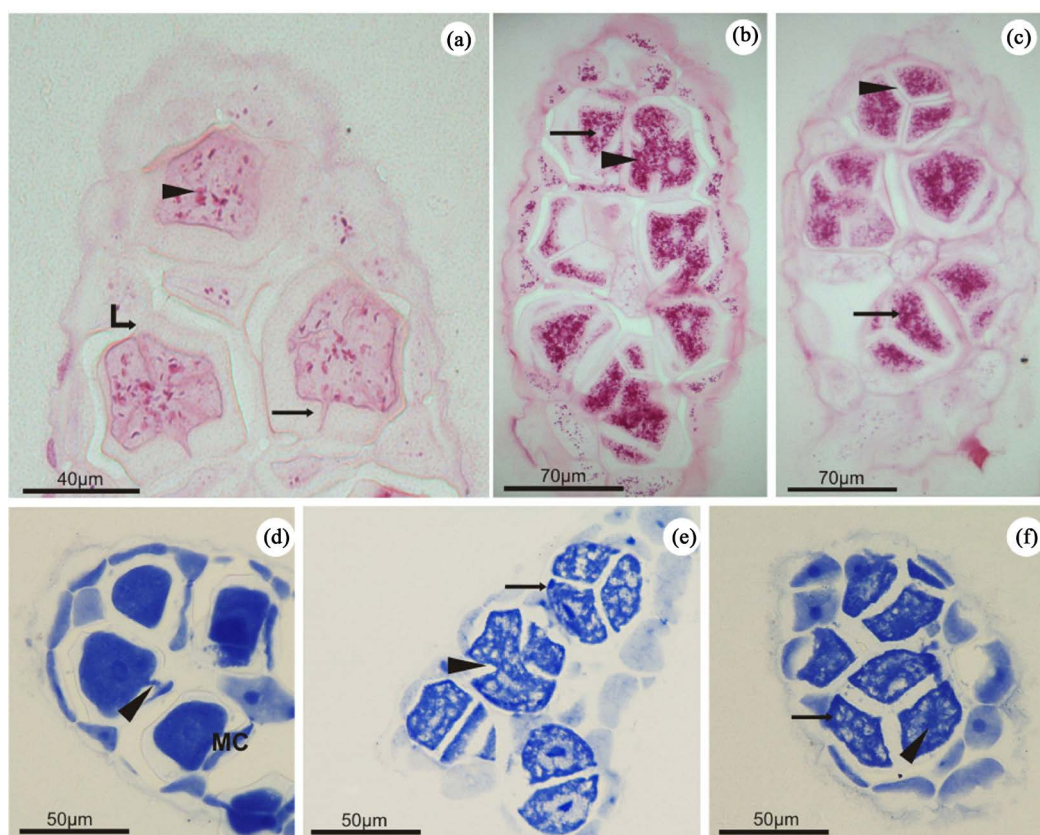


Figure 2. Light microscopy of *Bostrychia radicans*. (a)-(c) Longitudinal sections of stichidia stained with PAS. (a) Young tetrasporangium showing the cell wall (curved arrow), slightly positive to PAS. Note the small amount of starch grains in the cytoplasm (arrowhead) and the presence of a pit connection between the basal cell and the tetrasporangium (arrow). (b). Tetrasporangia showing advanced stages of maturation and revealing strong positive reaction to PAS in the cytoplasm (arrowhead). The cytoplasmic spaces with negative reaction indicate the location of the nuclei (arrow). (c) Mature tetrasporangia exhibiting strong positive reaction to PAS (arrow) and complete cellular division (arrowhead). (d)-(f) Longitudinal sections of stichidia stained with CBB. (d) Young tetrasporangia positively reacted to CBB, highlighting the pit connection (arrowhead) with its basal cell (BC). Note the strong positive reaction of the nuclei (arrow) and the dense cytoplasm. (e) Tetrasporangia at more advanced stages of maturation with wholly or partly divided cytoplasm (arrowhead). The cytoplasm was CBB-positive (arrow). (f) Totally divided mature tetrasporangium with an evident nucleus (arrowhead). The negatively stained regions indicate the presence of floridean starch grains (arrow).

involved in various metabolic pathways. Thus, when stained with CBB, it was possible to observe a homogeneous distribution pattern of proteins in the cytoplasm of the young tetrasporangia (**Figure 2(d)**). This indicates an intense proliferation of organelles and characterizes an active cytoplasm, which is a typical feature of maturing cells. In contrast, proteins in mature tetrasporangia are weakly marked, and the cytoplasm presents heterogeneously (**Figure 2(e)** and **Figure 2(f)**). This results from an increasing production of starch grains which occurs in parallel and occupies most parts of the cytoplasm. As a consequence, at this stage, the organelles lose their homogeneous distribution, as observed in the early phases, and are clustered in some regions of the cell in a random way. In addition, the nuclei of both young and mature tetrasporangia were visible and clearly CBB-positive (**Figures 2(d)-(f)**).

3.2. Confocal Microscopy

When the samples were analyzed by confocal microscopy, the peripheral cells of stichidia stained with DAPI presented one nucleus per cell (**Figure 3(a)**), but the tetrasporangium was not stained. Also, through chloroplast

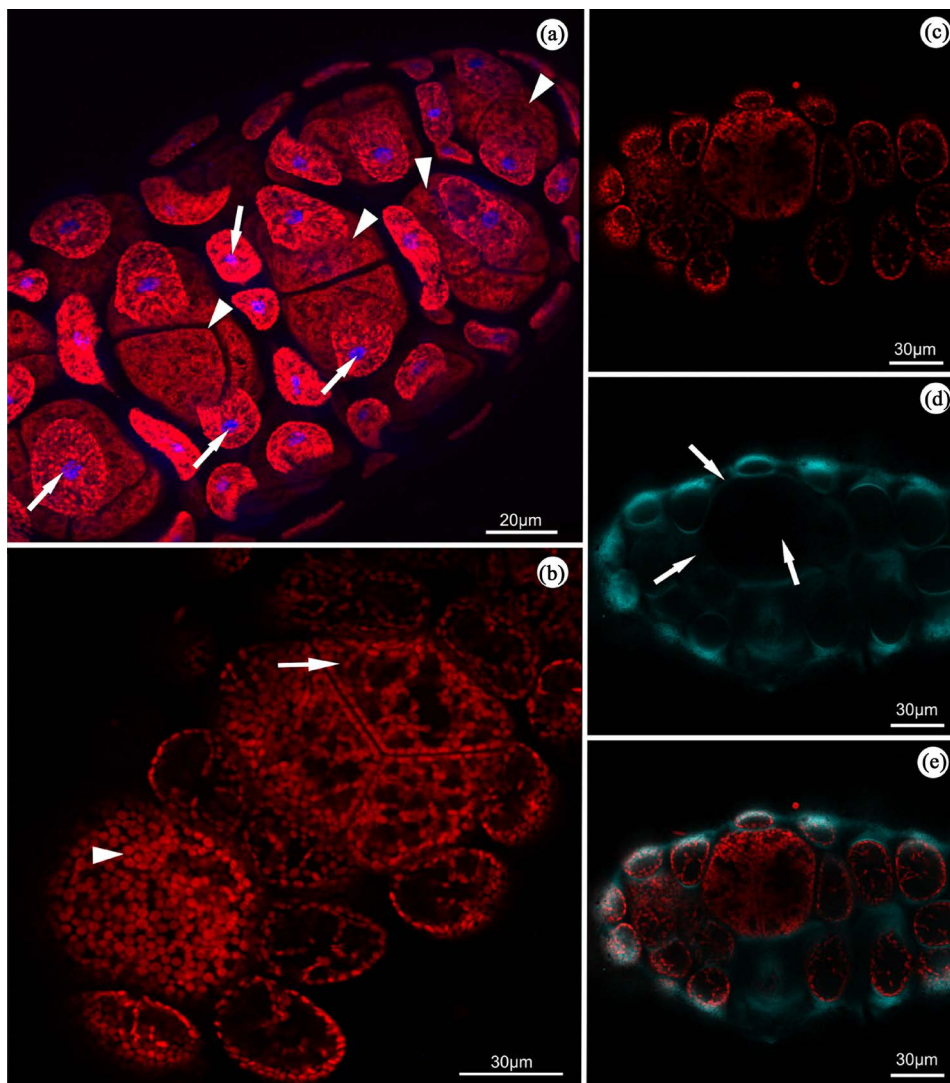


Figure 3. *B. radicans* stichidia observed under confocal microscopy. (a) The structure of stichidia with stained nuclei (blue) in the peripheral cells (arrows) and visualization of the tetrasporangium (arrowheads) in the central region. (b) Chloroplasts distributed homogeneously in young tetrasporangium (arrowheads) and heterogeneously in peripheral cells (arrows). (c) Autofluorescence of the chloroplasts. (d) Marking cell wall with calcofluor (blue-green), indicating lower amount of cellulose in tetrasporangium (arrows). (e) Overlay of images (c) and (d), with autofluorescence of chloroplasts and cell wall.

autofluorescence, we could observe that the chloroplasts in the young tetrasporangium are distributed homogeneously, while in the mature tetrasporangium and vegetative cells of stichidia, they were disposed heterogeneously (**Figure 3(b)** and **Figure 3(c)**). When stichidia were stained with calcofluor, no staining could be seen around the tetrasporangium, indicating that the cell wall does not contain large amounts of cellulose; however, staining with this treatment could be observed in the vegetative cell walls located in the peripheral position (**Figure 3(d)** and **Figure 3(e)**).

3.3. Transmission Electron Microscopy

During the early stages of tetrasporogenesis, chloroplasts actively proliferated and showed a structural organization typical of red algae (**Figure 4(a)**). Among the thylakoids, it was possible to observe electron-dense structures formed by lipid droplets (**Figure 4(h)**). It was also possible to register the presence of phycobilisomes, which are structures containing the characteristic red algae accessory pigments attached to the thylakoid membranes (**Figure 4(b)**). Chloroplasts were often observed in close association with mitochondria. Numerous mitochondria showing tubular cristae were observed in variable sizes and were found near the chloroplasts (**Figure 4(c)**).

According to the cytochemical studies, specifically PAS reaction, young tetrasporangia presented a small amount of starch grains (**Figure 4(d)**) which were often observed close to chloroplasts and Golgi bodies. During the final stages of tetrasporangia maturation, the number of starch grains increased considerably (**Figure 4(e)**).

During cytokinesis, cell membrane invagination and cell wall deposition occur together. In this region, near the membrane, it was possible to observe electron-transparent vesicles, which possibly have a role in depositing materials for wall formation (**Figure 4(f)**). The different patterns visualized in *B. radicans* allowed characterization of the cell wall into three distinct layers: inner, middle and outer (**Figure 4(g)**). At the end of the maturation process, however, as a consequence of cellular growth, a compaction of the outer layer fibrils occurred (**Figure 4(h)**). This may represent a strategy which gives greater desiccation resistance under low tide conditions.

Young tetrasporangia remain connected to the basal cell by a pit connection until full cell division is complete. These pit connections are closed by an electron-dense protein mass called a pit plug which prevents organelle traffic between cells. This protein mass is presented in a convex shape and is covered by a single or multi-lamellar layer: the cap layers (**Figure 4(i)**).

During tetrasporogenesis, the most conspicuous organelle was the Golgi complex. It usually consists of several hypertrophic cisternae and dilated vesicles in the region of maturation (**Figure 4(j)**).

The nucleus revealed an irregular envelope in young tetrasporangia, probably caused by the presence of numerous perinuclearly distributed chloroplasts. Also evident was a large nucleolus exhibiting electron-dense portions together with other small electron-transparent areas. In addition, a diffused chromatin was observed, clearly indicating intense cellular activity (**Figure 4(k)**).

4. Discussion

Tetrasporogenesis in *Bostrychia radicans* begins with the differentiation and resultant increase in the volume of some pericentral cells of branches located in the most apical region. Ultrastructurally, the process is characterized by an increase in the number and size of some organelles, such as mitochondria and chloroplasts. These organelles are the energy-producing centers of the cell, and, as such, they are characterized by a strategic increase in metabolic activity required in reproductive cells. This differentiation process of the cortical cells into reproductive ones was also observed in *P. palmata* and *H. musciformis* [13] [16].

During the ontogenesis of *B. radicans* tetrasporangium, cell walls were composed mainly of polysaccharides. In all cells of red algae, the polysaccharides are the most frequent and important primary metabolites sulfated [31]. The presence of acid polysaccharides in the *B. radicans* cell wall gives this species apparent support against tidal variations and the long periods of desiccation common in mangrove environments. For algae living in the intertidal zone, such polysaccharides should protect against desiccation during low tide periods [15]. As a component of the walls of reproductive cells, acid polysaccharides, by their hygroscopic nature, play a fundamental role in spore release [8]. In addition, the remaining mucilage, as observed on the spore surface, is probably used in spore adhesion to the substrate.

Among the acid polysaccharides present in the cell wall, the sulfated groups might be viewed by the reaction of AB. The pH of the AB solution was adjusted to 0.5. Consequently, carboxyl groups did not dissociate, and

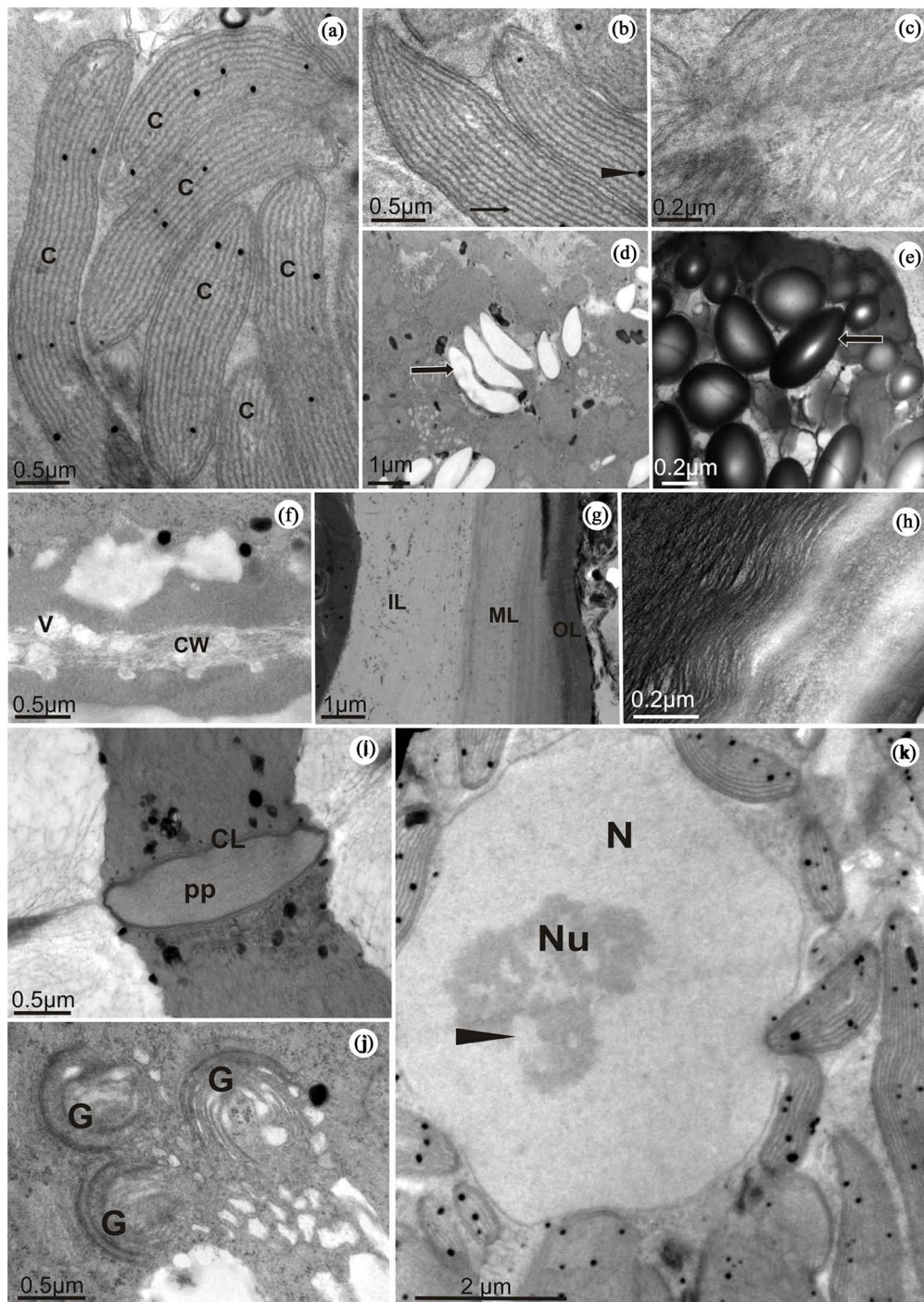


Figure 4. Tetrasporangia of *B. radicans* observed under transmission electron microscopy. (a) Perinuclear chloroplasts (C). (b) Chloroplasts with evident phycobilisomes adhered to the thylakoid surface (arrow). The arrowhead shows a plastoglobule. (c) Detail of a mitochondrion (M) showing its tubular cristae. (d) Starch grains (arrow) in a young tetrasporangium. (e) High amount of starch grains in a mature tetrasporangium (arrow). (f) Detail of the cell wall (CW) showing vesicles (V) depositing their content for use in cell wall formation. (g) Cell wall presenting different layers: inner layer (IL), middle layer (ML) and outer layer (OL). (h) Cell wall of a mature tetrasporangium showing its outer layer with compacted fibrils. (i) Pit connection between the tetrasporangium and the basal cell showing its pit plug (pp) and the cap layer (CL). (j) Hypertrophic Golgi bodies (G) surrounded by numerous free ribosomes. (k) Nucleus (N) with an evident electron-dense nucleolus (Nu) showing electron-transparent areas indicating the presence of diffuse chromatin (arrowhead). Note the presence of several chloroplasts surrounding the nucleus. Magnification 80,000 \times .

only the sulfated ones were marked. On the other hand, AY solution with a pH value of 2.5 exclusively reacts with carboxylated groups [10]. [2] also found this pattern in *Gracilaria* spp and *Gracilariopsis* sp sporogenesis, confirming results presented in this paper. However, studies on *Condrus crispus* by [32] suggest that polysaccharide sulfation also occurs in extracellular medium. The neutral polysaccharides were also observed in the cell wall by slightly positive reaction to PAS testing, indicating the presence of cellulose. This presence was higher in vegetative cells than in tetrasporangium, as demonstrated by the marking of calcofluor, which binds to cellulose. In ultrastructural analysis, the cell wall in *B. radicans* showed a texture characterized by microfibrils in layers with varying degrees of compression. However, when matured, a compression of the fibrils in the outer layer predominated in the samples. This compression of the fibrils may represent a greater resistance to desiccation during periods of low tide.

The cytoplasm of tetrasporangium showed a homogeneous pattern of protein distribution in young tetrasporangium, indicating an intense production of cell organelles. During this proliferation of organelles, the cytoplasm becomes very active, a feature typical of maturing cells. In the mature tetrasporangium, the marking of proteins becomes sparser. With the maturation of tetrasporangium, there is a greater production of starch grains, which occupy more space within the cytoplasm, causing the organelles to become more clustered. This variable pattern in total protein distribution in reproductive cells was also observed during carposporogenesis in *Gracilaria caudata* J. Agardh, *Gracilaria mammillaris* (Montagne) M.A. Howe and *Gracilariopsis tenuifrons* (C.J. Bird & E.C. Oliveira) Fredericq & Hommersand [2].

In young tetrasporangia, the slight PAS reaction in the cytoplasm indicated that the starch grains are gradually synthesized during the process of tetrasporangia ontogenesis. In TEM, the starch grains, while not having preferential localization, are observed most often in small amounts near the chloroplasts and Golgi bodies. The same phenomenon was found in *Membranoptera* sp (Harvey) Kuntze [33] and in *H. musciformis* [13]. Even floridean starch grains produced within chloroplasts can occur in the depressions of the external face of these organelles [22]. In algae species without pyrenoids, the starch grains are often found in proximity to nuclei, rough endoplasmic reticulum or other structures, suggesting the involvement of these organelles in the processes of reserve carbohydrate synthesis [34]. On the other hand, mature tetrasporangium, when treated with PAS, showed strong positive reaction throughout the cytoplasm, except in the nuclear region, corroborating the results obtained in confocal and ultrastructural analysis. This was attributed to the high rate of synthesis of starch grains at the end stage of maturation. This important starch accumulation can be attributed to the fact that a large amount of reserves will be used by released tetraspores as the main energy source for germination. This gradual deposition of starch grains during sporogenesis was also observed in *C. crispus* [26], *Palmaria palmata* (L.) O. Kuntze [16] and *H. musciformis* [4].

Chloroplasts in the cytoplasm present a typical characteristic of red algae, showing variations in size and shape, but predominantly elongated. The ultrastructural organization of chloroplasts is considered an important feature for the taxonomy of algae, but in the red algae, such ultrastructural organization is not associated with the thylakoid [2]. This organelle was often observed in perinuclear and peripheral regions of mature tetrasporangium. The presence of electron-dense structures among the thylakoids indicated that it was possibly formed by lipid droplets, which can be compared to plastoglobules described for *H. rubra* [16] and *H. musciformis* [13]. The presence of chloroplasts near the mitochondria can be compared to their arrangement in *P. palmata*, as described by [16], who interpreted it as a mechanism to increase the metabolic interaction between these organelles.

In a general, Golgi bodies consist of numerous dictyosomes, compounds of cisterns with small flattened vesicles which polarize in the face of maturation. The vesicles that are derived from Golgi bodies are involved in concentration and transport of material that are used to form the cell wall [2]. In *B. radicans*, as well as in other species studied by [2], the Golgi bodies become hypertrophic with the development of spores, producing a large number of cisterns and vesicles with diverse material. According to [16], the Golgi bodies are the main sources of mucilaginous material. This mucilaginous content is released through the fusion of vesicles with the cell membrane.

The nucleus is central to the young tetrasporangium and has diffuse chromatin and a large nucleolus, suggesting high metabolic activity during tetrasporangium maturation. However, the process of mitosis was not observed during the maturation of *B. radicans* tetrasporangia, suggesting that nuclear division is an event that occurs rapidly compared to cytokinesis. On the other hand, cytokinesis is a slow process and can be accompanied by ultrastructural studies. The grooves of invagination of the membrane, corresponding to the second meiotic

division, are accompanied by deposition of cell wall, as was also observed in tetrasporogenesis of the *P. palmata* [16] and *H. musciformis* [13].

At the end of the maturation process, each differentiated tetrasporangium was characterized by the presence of a large centrally located nucleus, as well as a great amount of starch grains, surrounded by a thin cell wall. This cell wall is characteristically thinner than those surrounding the initial tetrasporangia which undergo maturation. The mature cells are especially rich in organelles and reserve material, which are basic requirements for the initial germination events.

5. Conclusion

We concluded that tetrasporogenesis in *B. radicans* can be characterized by the proliferation of many organelles, especially chloroplasts, starch grains and Golgi bodies, as determined by performing cytochemical, structural and ultrastructural analyses under light, confocal, and transmission electron microscopy.

Acknowledgements

The authors would like to acknowledge the staff of the Central Laboratory of Electron Microscopy (LCME), Federal University of Santa Catarina, Florianópolis, Santa Catarina, Brazil, for the use of their scanning and transmission electron microscope. This study was supported in part by the Conselho Nacional de Desenvolvimento Científico e Tecnológico (CAPES, Brazil), Conselho Nacional de Desenvolvimento Científico e Tecnológico (CNPq, Brazil), and Fundação de Apoio à Pesquisa Científica e Tecnológica do Estado de Santa Catarina (FAPESC).

Conflict of Interest

The authors declare that they have no conflict of interest.

References

- [1] Fortes, A.C.M. (1992) Estudo taxonômico e aspectos ecológicos das Rhodophytano manguezal da Ilha de Santos (Complexo Estuarino Piauí—Fundo_Real, Sergipe. Dissertation, Univerdidade Federal Rural de Pernambuco.
- [2] Bouzon, Z.L. and Ouriques, L.C. (1999) Occurrence and Distribution of Bostrychia and Caloglossa (Rhodophyta, Ceramiales) in the Ratonés River Mangrove, Florianópolis—SC, Brazil. *Ínsula*, **28**, 43-52.
- [3] Zuccarello, C.G. and West, J.A. (1995) Hybridization Studies in *Bostrychia*. 1: *B. radicans* (Rhodomelaceae, Rhodophyta) from Pacific and Atlantic North America. *Phycological Research*, **43**, 233-240. <http://dx.doi.org/10.1111/j.1440-1835.1995.tb00029.x>
- [4] Karsten, U., West, J.A., Zuccarello, G. and Kirst, G.O. (1994) Physiological Ecotypes in the Marine Alga *Bostrychia radicans* (Ceramiales, Rhodophyta) from the East Coast of the U.S.A. *Journal of Phycology*, **30**, 174-182. <http://dx.doi.org/10.1111/j.0022-3646.1994.00174.x>
- [5] Kim, G.H., Shim, J.B., Klochkova, T.A., West, J.A. and Zuccarello, G.C. (2008) The Utility of Proteomics in Algal Taxonomy: *Bostrychia radicans Moritziana* (Rhodomelaceae, Rhodophyta) as a Model Study. *Journal of Phycology*, **44**, 1519-1528. <http://dx.doi.org/10.1111/j.1529-8817.2008.00592.x>
- [6] Zuccarello, G.C. and West, J.A. (2003) Multiple Cryptic Species: Molecular Diversity and Reproductive Isolation in the *Bostrychia radicans/B. moritziana* Complex (Rhodomelaceae, Rhodophyta) with Focus on North American Isolates. *Journal of Phycology*, **39**, 948-959. <http://dx.doi.org/10.1046/j.1529-8817.2003.02171.x>
- [7] Hadlich, R.M. and Bouzon, Z.L. (1985) Contribuição ao levantamento taxonômico das algas marinhas betônicas so mangue do Itacorubi—Florianópolis—Ilha de Santa Catarina—Brasil—II Rhodophyta. *Ínsula*, **15**, 89-116.
- [8] McCully, M. (1970) The Histological Localization of the Structural Polysaccharides of Seaweeds. *Annals of the New York Academy of Sciences*, **175**, 702-711. <http://dx.doi.org/10.1111/j.1749-6632.1970.tb45186.x>
- [9] Tripodi, G. (1971) The Fine Structure of the Cystocarp in the Red Alga *Polysiphonia sertularioides* (Grat.) J. Ag. *Journal of Submicroscopic Cytology*, **3**, 71-79.
- [10] Ramarao, K.R. (1970) Studies on Growth Cycle Anphycocolloid Corente in *Hypnea musciformis* (Wulf) Lamouroux. *Botanica Marina Berlin*, **13**, 163-165.
- [11] Saito, R.M. and Oliveira, E.C. (1990) Chemical Screening of Brazilian Marine Algae Producing Carrageenans. *Hydrobiologia*, **204-205**, 585-588. <http://dx.doi.org/10.1007/BF00040291>

- [12] Diannelidis, B.E. and Kristen, U. (1988) Comparative Histochemical Studies of Reproductive and Gametophytic Tissue of Marine Red Algae by Means of Fluorescent and Light Microscopy. *Botanica Marina*, **31**, 163-170. <http://dx.doi.org/10.1515/botm.1988.31.2.163>
- [13] Bouzon, Z.L. (2006) Histoquímica e ultra-estrutura da ontogênese dos tetrasporângios de *Hypnea musciformis* (Wulfen) J. V. Lamour. (Gigartinales, Rhodophyta). *Revista Brasileira de Botânica*, **29**, 229-238. <http://dx.doi.org/10.1590/S0100-84042006000200004>
- [14] Kugrens, P. and West, J.A. (1972) Ultrastructure of Tetrasporogenesis the Parasitic Red Alga *Levringiella gardneri* (Setchell) Kylin. *Phycologia*, **8**, 370-383.
- [15] Scott, J. and Dixon, P.S. (1973) Ultrastructure of Tetrasporogenesis in the Marine Red Alga *Ptilota hypnoides*. *Journal of Phycology*, **9**, 29-46. <http://dx.doi.org/10.1111/j.0022-3646.1973.00029.x>
- [16] Pueschel, C.M. (1979) Ultrastructure of Tetrasporogenesis in *Palmaria palmata* (Rhodophyta). *Journal of Phycology*, **15**, 409-424. <http://dx.doi.org/10.1111/j.1529-8817.1979.tb00713.x>
- [17] Pueschel, C.M. (1980) Evidence for Two Classes of Microbodies in Meiocytes of the Red Algae *Palmaria palmate*. *Protoplasma*, **104**, 273-282. <http://dx.doi.org/10.1007/BF01279772>
- [18] Santisi, S. and De Masi, F. (1981) An Electron Microscopic Study on Tetrasporogenesis of the Parasitic Red Alga *Erythrocytis montagnei* (Der. and Sol.) Silva. *Cytobios*, **31**, 163-178.
- [19] Pueschel, C.M. (1982) Ultrastructural Observation of Tetrasporangia and Conceptacles in *Hildenbrandia* (Rhodophyta, Hildenbrandiales). *British Phycological Journal*, **17**, 333-341. <http://dx.doi.org/10.1080/00071618200650331>
- [20] Vesk, M. and Borowitzka, M. (1984) Ultrastructure of Tetrasporogenesis in the Coralline Alga *Haliptilon cuvieri* (Rhodophyta). *Journal of Phycology*, **20**, 501-515. <http://dx.doi.org/10.1111/j.0022-3646.1984.00501.x>
- [21] Tsekos, I., Schnepf, E. and Makrantonakis, A. (1985) The Ultrastructure of Tetrasporogenesis in the Marine Red Alga *Chondria tenuissima* (Good. Et Woodw.) (Cerariales, Rhodomelaceae). *Annals of Botany*, **55**, 607-619.
- [22] Delivopoulos, S.G. (2002) Ultrastructure of Trichoblasts in the Red Alga *Osmundea spectabilis* var. *spectabilis* (Rhodomelaceae, Cerariales). *European Journal of Phycology*, **37**, 329-338. <http://dx.doi.org/10.1017/S0967026202003748>
- [23] Delivopoulos, S.G. (2004) Ultrastructure of Tetrasporogenesis in the Red Alga *Rhodymenia californica* var. *attenuate* (Rhodymeniaceae, Rhodymeniales, Rhodophyta). *Botanica Marina*, **47**, 222-230. <http://dx.doi.org/10.1515/BOT.2004.023>
- [24] Bouzon, Z.L., Miguens, F. and Oliveira, E.C. (2000) Male Gametogenesis in the Red Algae *Gracilaria* and *Gracilariopsis* (Rhodophyta, Gracilariales). *Cryptogamie Algologie*, **21**, 33-47. [http://dx.doi.org/10.1016/S0181-1568\(00\)00103-3](http://dx.doi.org/10.1016/S0181-1568(00)00103-3)
- [25] Gahan, P.B. (1984) Plant Histochemistry and Cytochemistry: An Introduction. Academic Press, London.
- [26] Gordon, E.M. and McCandless, E.L. (1973) Ultrastructure and Histochemistry of *Chondrus crispus* Stack. *Proceedings of Nova Scotia Institute Science*, **27**, 111-133.
- [27] Gant, E. (1980) Handbook of Phycological Methods. Phycological Society of America, London.
- [28] Sheahan, M.B., Staiger, C.J., Rose, R.J. and McCurdy, D.W. (2004) A Green Fluorescent Protein Fusion to Actin-Binding Domain 2 of Arabidopsis Fimbrin Highlights New Features of a Dynamic Actin Cytoskeleton in Live Plant Cells. *Plant Physiology*, **136**, 3968-3978. <http://dx.doi.org/10.1104/pp.104.049411>
- [29] Hepler, P.K. and Gunning, B.E.S. (1998) Confocal Fluorescence Microscopy of Plant Cells. *Protoplasma*, **201**, 121-157. <http://dx.doi.org/10.1007/BF01287411>
- [30] Reynolds, E.S. (1963) The Use of Lead Citrate at High pH as an Electron-Opaque Stain in Electron Microscopy. *Journal Cell Biology*, **17**, 208-212. <http://dx.doi.org/10.1083/jcb.17.1.208>
- [31] Carvalho, L.R. and Roque, N. (1996) Fenóis halogenados e/ou sulfatados de macroalgas marinhas. *Química Nova*, **23**, 757-763. <http://dx.doi.org/10.1590/S0100-40422000000600009>
- [32] Claire, J.W. and Dawes, C. (1976) An Autoradiographic and Histochemical Localization of Sulfated Polysaccharides in *Eucheuma nudum* (Rhodophyta). *Journal of Phycology*, **12**, 368-375.
- [33] McDonald, K. (1972) The Ultrastructure of Mitosis in the Marine Red Alga *Membranoptera platyphylla*. *Journal of Phycology*, **8**, 156-166. <http://dx.doi.org/10.1111/j.1529-8817.1972.tb01556.x>
- [34] Pueschel, C.M. (1990) Cell Structure. In: Cole, K.M. and Sheath, R.G., Eds., *Biology of the Red Algae*, Cambridge University Press, New York, 517 p.

List of Abbreviations

DAPI: 4',6-diamidino-2-phenylindole

AB: Alcian Blue

AY: Alcian Yellow

CBB: Coomassie Brilliant Blue

LM: Light Microscopy

PAS: Periodic Acid-Schiff

MET: Transmission Electron Microscopy